TABLE 3. (*continued*).

Gene	Exon No.	Length (bp)	Name	Forward Primer	Name	Reverse Primer	Size (bp)
	4	387	MP4aF	CCCTCTTAGAAGATTCCTGACTTA	MP4aR	ACACTCCACTGGTTGCCAT	249
			MP4bF	ATGAACAGCCTCAGCAGGA	MP4bR	GCAAAAGCTTTCGATGGTTA	316
	5	123	MP5F	GGAGGCAATATCAACATCTTCA	MP5R	TGCTTGAGGTTGAAACAGTTAAG	248
	6	120	MP6F	GCAAACAGCAATGCTAATTCA	MP6R	GAAATACTGCAACATGGCATG	250
	7	120	MP7F	CAGCTAGGGAATTATTTATCAGCA	MP7R	CAGGGATTGGACTTTATTCCA	279
	8	120	MP8F	ATATCCAAAGTAGTGGTGCACAA	P8R	TTCCTGGTTAAAACTAAATACCTAACA	235
	9	124	MP9F	TGCAAACAGAATCTGCCAGTA	MP9R	TTTGGCTTGGTAAGACCAGAA	265
	10	196	MP10F	CTTACCAAGCCAAACTGCTAACTA	MP10R	AACAAACTCCCATCTTTCTCAATAG	289
	11	162	MP11F	AAAGCATAGAAACTCCAATGCA	MP11R	AGGTAACAATATTCTTTGGCTGACT	281
ELOVL4	1	100	MP1F	CCGCGGTTAGAGGTGTTC	MP1R	GAGACCAGGGGTCGGTGAC	281
	2	188	MP2aF	TTGAGACATCTTGATTCCTAGAAAG	MP2aR	AAGTTAAGCAAAACCATCCCA	252
			MP2bF	CTGGGTCCAAAGTGGATGAA	MP2bR	AGCTAACAGTTATGTCTGGGTACAA	213
	3	81	MP3F	GCAATTGGAATGCATGACA	MP3R	TTTCACAGATTGGGGCCTATA	304
	4	172	MP4aF	AAATGATTCCATGCCTTGTACA	MP4aR	AACGCAAGCAGTATATTCCTGA	330
			MP4b	TGGTGTTTATAACACGCTTTCC	MP4bR	CTCATTGCTTTCCACTGAACA	271
	5	128	MP5F	ATCTCGGTGGCTTACTGCTTA	MP5R	AATAAGTCGGGCTGGAGTCAACT	356
	6	276	MP6aF	TTGGGCCTGTGATAGCTATG	MP6aR	TTAGGCTCTTTGTATGTCCGAA	247
			MP6bF	CTCTAATTGCCTACGCAATCAG	MP6bR	GGGAGTTTTTCCTCACTGTCA	242
TIMP3	1	121	MP1F	AACTTTGGAGAGGCGAGCA	MP1R	CCTAAGCAGCGCTGCAGTC	233
	2	83	MP2F	TGAGATGCTGTTCCTGATGTG	MP2R	GGCTGGTGCTTAGACACACA	266
	3	112	MP3F	AGCAGTGGGATTATGGATCATAC	MP3R	ACATTTGGTGAGTCAGCTACTCA	267
	4	122	MP4F	TGGGCTAAGTGGGAACATAGTA	MP4R	GTTTCTAGGGCTGCAAGTCA	274
	5	198	MP5F	TACCATGGCAGATTCCATCA	MP5R	AGTTAGTGTCCGAGGGAAGCT	306

* Exon 2, 7, and 10 of the *VMD2* gene were screened for sequence variants only by direct sequencing.

Linkage Analysis

Linkage analysis was performed on DNA from 19 affected and 7 unaffected members of the pedigree. Individuals used for the analysis are indicated by asterisks in Figure 1. Human microsatellite markers linked to human macular degeneration loci were analyzed with monkey genomic DNA used as the template. Details of microsatellite markers and their primer sequences were obtained from the genome database. Microsatellite marker analysis was performed by two methods: Markers linked to candidate gene loci and included in a linkage mapping set (ver. 2.5MD10; Applied Biosystems, Inc. [ABI], Foster City, CA) were analyzed on the a DNA sequencer (model 3100; ABI) with fluorescence-labeled primers. Additional microsatellite markers were analyzed by ^{32}P dCTP incorporation into the amplified product.[41] Two-point linkage analysis was performed between the disease locus and microsatellite markers with the MLINK program of the LINKAGE package, as described elsewhere.[42,43] Linkage was assessed under the conditions of autosomal dominant inheritance of the disease trait with a frequency of 0.001 for the disease-causing allele, by using the affecteds-only model, as published earlier.[44] Linkage analysis was performed assuming equal frequencies for marker alleles. Haplotypes were constructed with genotypes of microsatellite markers according to their order on human chromosomes.

RESULTS

Clinical and Histologic Findings

Fundus photographs and FA of a 14-year-old female affected monkey (Fig. 1, monkey A) are shown in Figure 2. Fine, yellowish white dots were observed in the maculae (Figs. 2a–d), scattered in the peripheral retina along blood vessels in this monkey (Figs. 2a, 2b). However, in most cases, the locations of the lesions fell within the region centered on the fovea centralis with the same diameter as one optic disc. FA showed hyperfluorescence corresponding to these dots, except foveola (Figs. 2c, 2f). No abnormalities were found in the optic disc, retinal blood vessels, or choroidal vasculatures in any eyes examined. The amplitude and peak latency of both dark- and light-adapted ERG showed no alteration compared with normal control eyes, indicating that global rod or cone degeneration was absent. Histologic studies demonstrated that there were various-sized drusen, weakly stained by PAS (light purple), between the RPE and choriocapillaris in the macular region (Figs. 3a, 3b, asterisk). These drusen were strongly reactive with antibodies against complement C5 (Figs. 3c, 3d). This finding was consistent with the property of drusen reported in patients with AMD.[35] Accumulation of lipofuscin in RPE cells was also obvious by PAS (Figs. 3a, 3b, deep purple, arrows).

Mutation Analysis of the *ABCA4*, *VMD2*, *EFEMP1*, *TIMP3*, and *ELOVL4* Genes

To evaluate the involvement of the *ABCA4*, *VMD2*, *EFEMP1*, *TIMP3*, and *ELOVL4* genes in disease, we first determined the genomic sequence and the complete cDNA sequence of the orthologous genes in the monkey. Subsequently, these genes were screened for sequence variants in affected and unaffected monkeys in the pedigree, in addition to unrelated, unaffected animals by SSCP, or by DHPLC for the *ABCA4* gene, analysis and direct sequencing.

ABCA4. The monkey *ABCA4* gene consists of 50 exons, with its translation stop codon in exon 50, similar to the human gene. The complete 6819-bp cDNA encodes a protein of 2273 amino acids. *ABCA4* is a member of the superfamily of ATP-binding cassette (ABC) transporters, which are associated with membranes and transport various molecules across extra- and intracellular membranes of all cell types. ABC genes typically encode four domains that include two conserved ATP-binding domains and two domains with multiple transmembrane segments. Comparative sequence analysis revealed that the monkey ABCA4 protein was only 1.8% (41 amino acids) different from the human orthologue, whereas the sequence was identical in the two adenosine triphosphate (ATP)-binding domains. Five of the 41 nonconserved amino acids in the monkey protein (codons 223, 423, 1300, 1817, and 2255) involve polymorphisms in the human. Surprisingly, the Lys223Gln and Arg1300Gln changes reported to be associated with Stargardt disease in humans were observed in the homozygous state in

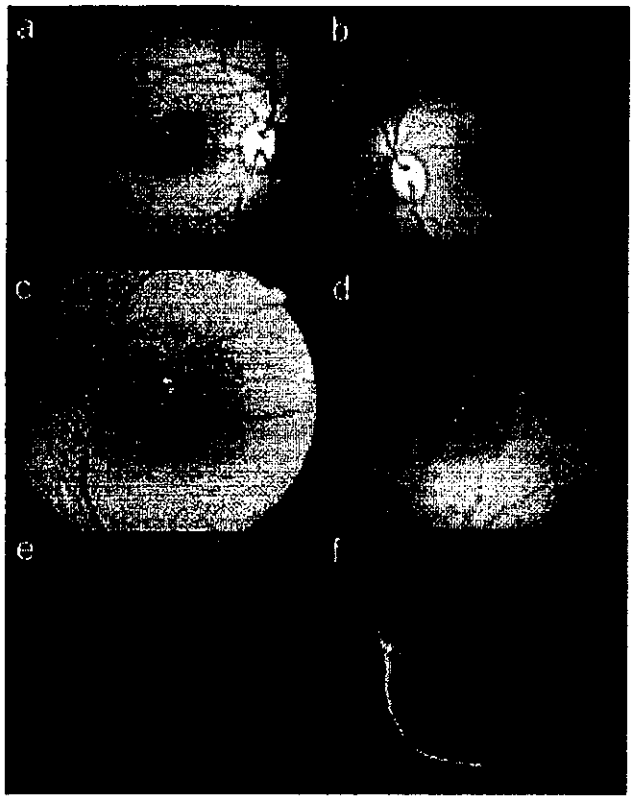

FIGURE 2. Fundus photographs and fluorescein angiogram (FA) of a 14-year-old female cynomolgus monkey (Fig. 1, monkey A) with macular degeneration, showing the right (**a**, **c**, **e**) and left (**b**, **d**, **f**) posterior poles. Fine *grayish white* or *yellowish white* dots were visible in the macula (**a**–**d**). The dots were observed in the peripheral retina along blood vessels in this monkey (**a**, **b**). These dots showed hyperfluorescence in FA except in the foveola (**e**, **f**). High-magnification of the macular region (**c**, **d**, **e**).

one normal control monkey (Fig. 1, monkey C). In addition, the mutation analysis revealed heterozygous amino acid changes at five positions—Leu424Val, Arg1017His, Val1114Ile, Ile1615Val, and Pro2238Gln—in both affected and normal monkeys. However, these missense variants did not segregate with the disease phenotype.

VMD2. The monkey *VMD2* gene consists of 11 exons, with its translation initiation codon in exon 2, as observed in its human orthologue. The complete cDNA was 2187 bp, encoding 585 amino acids. The *VMD2* gene encodes the bestrophin protein, which localizes to the basolateral plasma membrane of the RPE with the postulated function as an oligomeric chloride channel.[36,37] The hydropathy profile predicted that bestrophin contains four stretches of hydrophobic amino acids that function as transmembrane domains. Comparative sequence analysis demonstrated that monkey bestrophin had 19 amino acids different from its human homologue, and the four putative transmembrane domains are highly conserved. To date, 72 disease-associated nucleotide substitutions of the *VMD2* gene have been identified in patients with Best disease.[3,7,26] The mutation analysis of the *VMD2* gene in the monkey pedigree detected six amino acid sequence variants. A polymorphism (Val/Ile) was detected at codon 275 in the fourth transmembrane domain, which has also been reported in humans.[26] Four polymorphisms (Tyr465His, Thr542Met, Glu557Gln, and Thr566Ala) were detected in exon 10. These changes did not segregate with the disease. In addition, one nonsense mutation at codon 582 (Glu→Stop) in exon 11 was detected in two normal monkeys, whereas none of the examined six affected monkeys showed the change.

EFEMP1. The exon–intron gene structure of the monkey *EFEMP1* gene was also similar to the human *EFEMP1* gene. It was composed of 11 exons with its translation initiation codon in exon 2. The complete cDNA was 2034 bp, encoding 493 amino acids. Although the function of this gene remains unclear, this class of proteins is known to have characteristic sequence of repeated calcium-binding EGF-like domains.[4] The monkey *EFEMP1* cDNA was found to have six EGF repeats. Four EGF repeats (numbers 2–5) are encoded by single exons (exons 5–8), one EGF repeat (number 1) is encoded by three exons (exons 2–4), and EGF repeat number 6 is encoded by two exons (exons 9, 10). This finding is in agreement with one of the two transcriptional variants with a distinct 5′ untranslated region (UTR) described in its human homologue. Comparative sequence analysis demonstrated that the monkey *EFEMP1* has three amino acids different from that of the human, but the sequence in the entire region of six EGF repeats is completely conserved. In humans, a single mutation (Arg345Trp) that disrupts one of these domains is known to cause Malattia Leventinese.[4] No amino acid–changing polymorphisms were found in all the monkeys tested. Three single nucleotide polymorphisms (SNPs), that did not alter the amino acid sequence, were detected in exons 4, 5, and 10.

TIMP3. The monkey *TIMP3* gene consisted of five exons, similar to its human orthologue. The complete cDNA was 1887 bp in length, encoding 211 amino acids. *TIMP3* is the third member of the tissue inhibitors of metalloproteinase family, a group of zinc-binding endopeptidases involved in the degradation of the extracellular matrix. *TIMP3* has 12 cysteines characteristic of the TIMP family, which are proposed to form intramolecular disulfide bonds and tertiary structure for the functional properties of the mature protein. The predicted amino acid sequence of the monkey *TIMP3* gene was identical with the human orthologue, including the 12 cysteine residues. Mutations in the *TIMP3* gene are known to cause Sorsby's fundus dystrophy.[5] With a few exceptions,[38,39] most previously described mutations disrupt the disulfide bonds by changing residues into cysteines, leading to misfolding of the protein.[5,10] No coding sequence changes were detected in the *TIMP3* gene in monkeys by mutation screening.

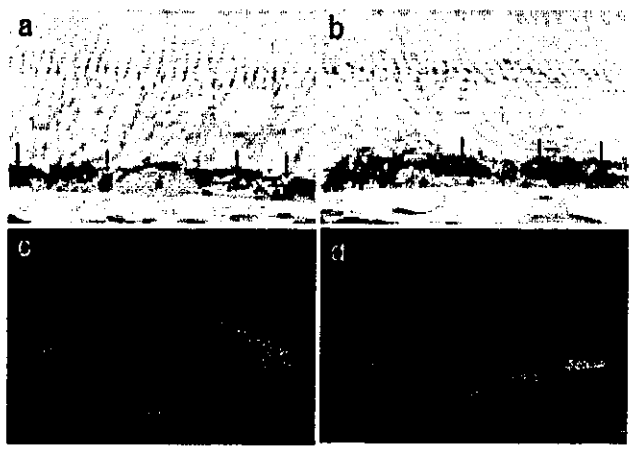

FIGURE 3. Drusen in the affected monkey retina. An affected 14-year-old male monkey (Fig. 1, monkey B). There were various-sized drusen, which were weakly stained by PAS (*), between the RPE and choriocapillaris (CC) (**a**, **b**). These drusen were strongly reactive with antibodies against complement C5 (*green* channel). Lipofuscin autofluorescence is shown (*red*) in the RPE (**c**, **d**). Accumulation of lipofuscin in RPE cells was also obvious by PAS (**a**, **b**, *arrows*).

TABLE 4. Two-Point Lod Scores between the Monkey Macular Degeneration Locus and Markers at the Human Macular Degeneration Loci

Markers	Distance from the Gene (CM)	Order on the Chromosome (M)	Lod Scores at θ									Exclusion ($Z = -2$)
			0	0.001	0.005	0.01	0.05	0.1	0.2	0.3	0.4	
CORD8		154.28										
D1S431	10.5	165	$-\varepsilon$	−2.116	−1.422	−1.128	−0.483	−0.248	−0.071	−0.01	0.006	0.001
D1S2635	0	154.28	$-\varepsilon$	−11.078	−7.598	−6.112	−2.773	−1.469	−0.392	0.019	0.119	0.075
D1S2715	−6.9	147.01	$-\varepsilon$	−7.7	−4.925	−3.747	−1.162	−0.232	0.388	0.464	0.299	0.03
D1S498	−10.6	144.94	$-\varepsilon$	−1.124	−0.439	−0.154	0.416	0.564	0.567	0.433	0.227	0.0001
ABCA4		94.1										
D1S188	−2.3	91.7	$-\varepsilon$	−6.139	−4.058	−3.175	−1.24	−0.541	−0.05	0.074	0.066	0.01
D1S2849	−1.2	92.9	$-\varepsilon$	−1.766	−1.075	−0.784	−0.166	0.032	0.133	0.119	0.067	
D1S2868	0.1	94	$-\varepsilon$	−14.824	−10.623	−8.809	−4.599	−2.846	−1.264	−0.522	−0.146	0.1
STGD3		80.5										
D6S1662	−2.67	77.83	$-\varepsilon$	−1.232	−0.544	−0.257	0.324	0.476	0.472	0.34	0.17	0.0
D6S1048	0.28	80.78	$-\varepsilon$	−0.063	0.614	0.889	1.38	1.416	1.172	0.79	0.362	0.0
D6S1596	7.1	87.6	$-\varepsilon$	−8.746	−5.965	−4.78	−2.138	−1.127	−0.319	−0.025	0.049	0.05
D6S1609	12.08	92.58	$-\varepsilon$	−7.326	−5.235	−4.34	−2.302	−1.475	−0.724	−0.349	0.131	0.05
DHRD		56.1										
D2S2230	3.9	60	$-\varepsilon$	−11.691	−8.209	−6.719	−3.349	−2.006	−0.842	−0.325	−0.084	0.1
D2S378	1.1	57.2	$-\varepsilon$	−9.268	−6.482	−5.29	−2.593	−1.517	−0.588	−0.186	−0.019	0.05
ARMD1		192.2										
D1S384	−2.11	190.09	$-\varepsilon$	−5.565	−3.486	−2.606	−0.696	−0.032	0.375	0.389	0.236	0.01
D1S413	2.1	194.1	$-\varepsilon$	−11.068	−7.59	−6.106	−2.784	−1.501	−0.46	−0.067	0.047	0.05
D1S2622	3.7	195.9	$-\varepsilon$	−1.961	−1.271	−0.982	−0.375	−0.185	−0.084	−0.066	−0.047	0.0
VMD2		61.5										
D11S1993	−2.3	59.2	$-\varepsilon$	−1.615	−0.925	−0.636	−0.032	0.151	0.224	0.181	0.1	0.0
D11S4174	1.4	62.9	$-\varepsilon$	−7.132	−5.026	−4.112	−1.979	−1.102	−0.368	−0.087	0.003	0.01
D11S4076	7.3	66.8	$-\varepsilon$	−5.617	−3.537	−2.656	−0.736	−0.061	0.364	0.385	0.231	0.01
Rhodopsin		130.6										
D3S3515	−4.01	126.59	$-\varepsilon$	−2.756	−1.379	−0.803	0.383	0.717	0.775	0.584	0.302	0.001
D3S3720	−2.8	127.8	$-\varepsilon$	−2.626	−1.247	−0.67	0.531	0.879	0.945	0.729	0.389	0.001
D3S1269	0.3	130.9	$-\varepsilon$	−11.566	−8.081	−6.588	−3.2.	−1.846	−0.7	−0.238	−0.062	0.05
Timp3		31.5										
D22S1162	7.05	38.55	$-\varepsilon$	−3.587	−2.203	−1.619	−0.365	0.055	0.291	0.276	0.159	0.005
D22S280	0	31.5	$-\varepsilon$	−4.051	−2.664	−2.075	−0.785	−0.321	−0.002	0.065	0.044	0.01
D22S273	−1	30.5	$-\varepsilon$	−1.878	−1.187	−0.896	−0.278	−0.078	0.026	0.025	0.004	0.0
CTRP5		118.7										
D11S4127	−1.6	117.1	$-\varepsilon$	−0.771	−0.088	0.192	0.73	0.827	0.719	0.495	0.244	0.0
D11S924	0.2	118.9	$-\varepsilon$	−1.424	−0.736	−0.449	0.137	0.298	0.322	0.232	0.113	0.0
D11S4129	4.18	121.58	$-\varepsilon$	−9.057	−6.275	−5.089	−2.435	−1.41	−0.566	−0.214	−0.054	0.05
STGD4		26.1										
D4S403	0	26.1	$-\varepsilon$	−16.798	−11.919	−9.83	−5.081	−3.159	−1.445	−0.633	−0.206	0.1
D4S391	1.2	27.3	$-\varepsilon$	−3.615	−2.231	−1.647	−0.392	0.026	0.255	0.234	0.13	0.005
CORD5	(Interval)	64.5										
D17S938	0	64.5	$-\varepsilon$	−16.296	−11.422	−9.339	−4.638	−2.776	−1.176	−0.466	−0.125	0.1
D17S796	0	64.5	$-\varepsilon$	−3.594	−2.209	−1.624	−0.358	0.075	0.324	0.305	0.176	0.0
MCDR1	(Interval)	98.1										
D6S434	4.3	102.4	$-\varepsilon$	−4.496	−3.103	−2.507	−1.163	−0.632	−0.183	−0.005	0.043	0.0
CORD9	(Interval)	47.6										
D8S1820	0	47.6	$-\varepsilon$	−11.981	−8.501	−7.014	−3.65	−2.277	−1.002	−0.385	−0.092	0.1

ELOVL4. We have reported cloning and characterization of the *ELOVL4* gene in the cynomolgus monkey.[11] Three mutations leading to truncation of the *ELOVL4* protein were reported in humans with Stargardt-like macular dystrophy[25,42] (Karen G, et al. *IOVS* 2004;45:ARVO E-Abstract 1766). Mutation analysis of monkeys with macular degeneration did not detect any amino acid–altering sequence changes. Silent polymorphisms were observed in exons 1, 3, and 4 of the *ELOVL4* gene.

Linkage Analysis of Candidate Gene Loci

The methodology we used to screen for mutations in the candidate genes could miss disease-associated changes that may be present in the promoter or intronic regions; therefore, linkage analysis was performed to exclude the five genes further. Moreover, the macular degeneration phenotype in the monkey pedigree could be caused by a single gene defect. In these cases, linkage analysis would be a comprehensive approach to confirm or exclude a particular gene locus. Microsatellite markers linked to the five candidate gene loci in addition to eight human macular degeneration loci—*ABCA4*, *VMD2*, *DHRD* (*EFEMP1*), *TIMP3*, *STGD3* (*ELOVL4*), Cone rod dystrophy-8 (*CORD-8*), age-related macular degeneration 1 (*ARMD1*, gene Hemicentin1), rhodopsin, *STGD4*, North Carolina macular degeneration (*MCDR1*), *CORD9*, late-onset retinal degeneration (*CTRP5*), and *CORD5* loci—were analyzed to test for linkage with the macular degeneration in the monkey pedigree. None of the tested loci gave significant positive lod scores (Table 4). We also constructed haplotypes using the genotype data of markers at the 13 loci. This analysis further supported the exclusion of these loci from being among those that might harbor the gene associated with macular degeneration in these monkeys.

Discussion

We report a detailed description of early-onset macular degeneration in cynomolgus monkeys and the exclusion of known genes responsible for macular degeneration in humans as a disease-associated gene in this animal model. Several forms of macular degeneration have been described in humans, including autosomal dominant, autosomal recessive, and X-linked modes of inheritance. The most common form of macular disease in humans is AMD. Major clinical characteristics of AMD are loss of central vision with RPE atrophy or exudation. The presence of subretinal deposits known as drusen is one of the early signs observed in AMD and several other macular degenerations. Recent studies suggest that the process of drusen formation includes inflammatory and immune-mediated events.[35] Immunohistochemical examinations have revealed that drusen contains activated complement factors. These molecules include C5, the cleavage product of C3 (C3b, iC3b, and C3dg), and the terminal complement complex C5b-9. Clinical and histologic studies of the affected monkeys showed the presence of drusen (Figs. 2, 3). Immunologic analysis demonstrated that drusen in monkeys had C5 as a component, suggesting that the nature of monkey drusen was similar to that reported in human AMD. At the same time, the onset of the disease in monkeys is at ~2 years of age; therefore, the monkey macular degeneration resembles early-onset human macular degeneration with drusen.

Comparison of the gene maps and chromosome painting data revealed a high degree of synteny and genome conservation between human and Macaque genomes.[43,44] Amplification of cynomolgus monkey DNA with human microsatellite marker primers and sequence analysis revealed that not only the sequences flanking the microsatellite repeat regions but also the polymorphic nature of these repeats is conserved between human and monkey genomes (data not shown). Comparative studies on human and chimpanzee genomes have shown the same average heterozygosity at microsatellite marker loci and conserved genetic distance between markers.[45] Molecular cloning of monkey orthologues of the human *ABCA4*, *VMD2*, *EFEMP1*, *TIMP3*, and *ELOVL4* genes further demonstrated the high conservation between the human and macaque genomes not only in the organization of the gene structure, but also at the sequence level. Considering the high conservation between human and macaque genomes, human macular degeneration loci can be considered plausible candidates for identification of the gene associated with macular degeneration in the monkeys. We tested this hypothesis using microsatellite markers linked to human macular degeneration loci and successfully amplified microsatellites in the monkey DNA with human primers. However, we failed to establish linkage with the tested loci, and the subsequent haplotype analysis further confirmed this finding. Therefore, the macular degeneration locus in the monkey pedigree is not likely to be associated with the regions of the monkey genome that are syntenic to human genomic regions comprising the 13 macular disease loci tested. Mutation analysis of candidate genes also supported the exclusion of the *ABCA4*, *VMD2*, *EFEMP1*, *TIMP3*, and *ELOVL4* genes. The analyses detected five- and six-amino-acid substitutions in the *ABCA4* and *VMD2* genes, respectively. Some silent nucleotide substitutions or intronic sequences changes, such as small insertions/deletions, SNPs, and variations of short tandem repeats were observed in the *EFEMP1*, *TIMP3*, and *ELOVL4* genes. All these sequence variants did not segregate with the disease phenotype in the extended pedigree. Hence, these changes were interpreted as benign polymorphisms.

In the *ABCA4* sequence of a normal monkey, we found two amino acid replacements (K223Q and R1300Q) that are associated with Stargardt disease in humans. Because of the extensive conservation between the monkey and human gene sequences, one would expect these amino acid changes to have similar disease-associated effects in monkeys. One explanation of this discrepancy could be that K223Q and R1300Q are not causing the disease phenotype in humans, but rather represent markers linked to disease-causing mutations somewhere else in the gene. Alternatively, the disease-causing effect of these amino acid changes on the function of the human ABCA4 protein could be eliminated or compensated for by other differences in the monkey protein. Comparative analysis of the monkey and human genes may provide clues for understanding the molecular pathogenesis caused by *ABCA4* variation. In the *VMD2* gene sequence of normal monkeys, we found a nonsense mutation at codon 582. The change is located at the fourth residue from the C terminus. Bestrophin was shown to form oligomeric chloride channels in cell membranes.[37] The C-terminal cytosolic tail, encoded by exons 10 and 11, has been reported not to be essential for the protein's function. Moreover, although 72 nucleotide substitutions have been identified in Best disease to date,[3,7,26] none of them is reported in exons 10 and 11. Hence, the deletion of four amino acids from the C-terminal end of the protein could be considered not to be associated with the disease.

In summary, we demonstrated that none of the 13 human macular degeneration loci tested were involved in causing the macular degeneration phenotype observed in the monkey pedigree. These results demonstrate the need for additional studies to identify the genetic locus associated with the phenotype in these monkeys and to understand the genetic defect underlying the disease. Identification of the gene responsible for this specific macular degeneration phenotype not only defines a new candidate locus for human macular degeneration, but also provides a primate animal model that can be extensively studied for elucidation of the mechanisms, diagnosis, prophylaxis, and treatment of macular degenerations, including AMD.

References

1. Michaelides M, Hunt DM, Moore AT. The genetics of inherited macular dystrophies. *J Med Genet.* 2003;9:641–650.
2. Allikmets R, Singh N, Sun H, et al. A photoreceptor cell-specific ATP-binding transporter gene (ABCR) is mutated in recessive Stargardt macular dystrophy. *Nat Genet.* 1997;3:236–246.
3. Petrukhin K, Koisti MJ, Bakall B, et al. Identification of the gene responsible for Best macular dystrophy. *Nat Genet.* 1998;3:241–247.
4. Stone EM, Lotery AJ, Munier FL, et al. A single EFEMP1 mutation associated with both Malattia Leventinese and Doyne honeycomb retinal dystrophy. *Nat Genet.* 1999;2:199–202.
5. Weber BH, Vogt G, Pruett RC, Stohr H, Felbor U. Mutations in the tissue inhibitor of metalloproteinases-3 (TIMP3) in patients with Sorsby's fundus dystrophy. *Nat Genet.* 1994;4:352–356.
6. Zhang K, Kniazeva M, Han M, et al. A 5-bp deletion in ELOVL4 is associated with two related forms of autosomal dominant macular dystrophy. *Nat Genet.* 2001;1:89–93.
7. Marquardt A, Stohr H, Passmore LA, et al. Mutations in a novel gene, VMD2, encoding a protein of unknown properties cause juvenile-onset vitelliform macular dystrophy (Best's disease). *Hum Mol Genet.* 1998;9:1517–1525.
8. Bernstein PS, Tammur J, Singh N, et al. Diverse macular dystrophy phenotype caused by a novel complex mutation in the *ELOVL4* gene. *Invest Ophthalmol Vis Sci.* 2001;13:3331–3336.
9. Dithmar S, Curcio CA, Le NA, Brown S, Grossniklaus HE. Ultrastructural changes in Bruch's membrane of apolipoprotein E-deficient mice. *Invest Ophthalmol Vis Sci.* 2000;8:2035–2042.
10. Mata NL, Tzekov RT, Liu X, et al. Delayed dark-adaptation and lipofuscin accumulation in abcr+/− mice: implications for involvement of ABCR in age-related macular degeneration. *Invest Ophthalmol Vis Sci.* 2001;8:1685–1690.

11. Rakoczy PE, Zhang D, Robertson T, et al. Progressive age-related changes similar to age-related macular degeneration in a transgenic mouse model. *Am J Pathol.* 2002;4:1515–1524.
12. Stafford TJ. Maculopathy in an elderly sub-human primate. *Mod Probl Ophthalmol.* 1974;0:214–219.
13. El-Mofty A, Gouras P, Eisner G, Balazs EA. Macular degeneration in rhesus monkey (Macaca mulatta). *Exp Eye Res.* 1978;4:499–502.
14. Hope GM, Dawson WW, Engel HM, et al. A primate model for age related macular drusen. *Br J Ophthalmol.* 1992;1:11–16.
15. Nicolas MG, Fujiki K, Murayama K, et al. Studies on the mechanism of early onset macular degeneration in cynomolgus monkeys. II. Suppression of metallothionein synthesis in the retina in oxidative stress. *Exp Eye Res.* 1996;4:399–408.
16. Nicolas MG, Fujiki K, Murayama K, et al. Studies on the mechanism of early onset macular degeneration in cynomolgus (Macaca fascicularis) monkeys. I. Abnormal concentrations of two proteins in the retina. *Exp Eye Res.* 1996;3:211–219.
17. Suzuki MT, Terao K, Yoshikawa Y. Familial early onset macular degeneration in cynomolgus monkeys (Macaca fascicularis). *Primates.* 2003;3:291–294.
18. Klaver CC, Wolfs RC, Assink JJ, et al. Genetic risk of age-related maculopathy: population-based familial aggregation study. *Arch Ophthalmol.* 1998;12:1646–1651.
19. Seddon JM, Ajani UA, Mitchell BD. Familial aggregation of age-related maculopathy. *Am J Ophthalmol.* 1997;2:199–206.
20. Meyers SM, Greene T, Gutman FA. A twin study of age-related macular degeneration. *Am J Ophthalmol.* 1995;6:757–766.
21. Tuo J, Bojanowski CM, Chan CC. Genetic factors of age-related macular degeneration. *Prog Retin Eye Res.* 2004;2:229–249.
22. Abecasis GR, Yashar BM, Zhao Y, et al. Age-related macular degeneration: a high-resolution genome scan for susceptibility loci in a population enriched for late-stage disease. *Am J Hum Genet.* 2004;3:482–494.
23. Ayyagari R, Zhang K, Hutchinson A, et al. Evaluation of the ELOVL4 gene in patients with age-related macular degeneration. *Ophthalmic Genet.* 2001;4:233–239.
24. Allikmets R. Further evidence for an association of ABCR alleles with age-related macular degeneration: the International ABCR Screening Consortium. *Am J Hum Genet.* 2000;2:487–491.
25. Felbor U, Doepner D, Schneider U, Zrenner E, Weber BH. Evaluation of the gene encoding the tissue inhibitor of metalloproteinases-3 in various maculopathies. *Invest Ophthalmol Vis Sci.* 1997; 6:1054–1059.
26. Lotery AJ, Munier FL, Fishman GA, et al. Allelic variation in the VMD2 gene in best disease and age-related macular degeneration. *Invest Ophthalmol Vis Sci.* 2000;6:1291–1296.
27. Honjo S. The Japanese Tsukuba Primate Center for Medical Science (TPC): an outline. *J Med Primatol.* 1985;2:75–89.
28. Marmor MF, Zrenner E. Standard for clinical electroretinography (1999 update): International Society for Clinical Electrophysiology of Vision. *Doc Ophthalmol.* 1998;2:143–156.
29. Dockhorn-Dworniczak B, Dworniczak B, Brommelkamp L, et al. Non-isotopic detection of single strand conformation polymorphism (PCR-SSCP): a rapid and sensitive technique in diagnosis of phenylketonuria. *Nucleic Acids Res.* 1991;9:2500.
30. Liu W, Smith DI, Rechtzigel KJ, Thibodeau SN, James CD. Denaturing high performance liquid chromatography (DHPLC) used in the detection of germline and somatic mutations. *Nucleic Acids Res.* 1998;6:1396–1400.
31. Griesinger IB, Sieving PA, Ayyagari R. Autosomal dominant macular atrophy at 6q14 excludes CORD7 and MCDR1/PBCRA loci. *Invest Ophthalmol Vis Sci.* 2000;1:248–255.
32. Terwilliger JD, Ott J. *Handbook of Human Genetic Linkage.* Baltimore, MD: The Johns Hopkins University Press; 1994.
33. Otto J. *Analysis of Human Genetic Linkage.* Baltimore, MD: The Johns Hopkins University Press; 1999.
34. Khani SC, Karoukis AJ, Young JE, et al. Late-onset autosomal dominant macular dystrophy with choroidal neovascularization and nonexudative maculopathy associated with mutation in the RDS gene. *Invest Ophthalmol Vis Sci.* 2003;8:3570–3577.
35. Mullins RF, Russell SR, Anderson DH, and Hageman GS. Drusen associated with aging and age-related macular degeneration contain proteins common to extracellular deposits associated with atherosclerosis, elastosis, amyloidosis, and dense deposit disease. *FASEB J.* 2000;7:835–846.
36. Marmorstein AD, Marmorstein LY, Rayborn M, et al. Bestrophin, the product of the Best vitelliform macular dystrophy gene (VMD2), localizes to the basolateral plasma membrane of the retinal pigment epithelium. *Proc Natl Acad Sci USA.* 2000;23: 12758–12763.
37. Sun H, Tsunenari T, Yau KW, Nathans J. The vitelliform macular dystrophy protein defines a new family of chloride channels. *Proc Natl Acad Sci USA.* 2002;6:4008–4013.
38. Tabata Y, Isashiki Y, Kamimura K, Nakao K, Ohba N. A novel splice site mutation in the tissue inhibitor of the metalloproteinases-3 gene in Sorsby's fundus dystrophy with unusual clinical features. *Hum Genet.* 1998;2:179–182.
39. Langton KP, McKie N, Curtis A, et al. A novel tissue inhibitor of metalloproteinases-3 mutation reveals a common molecular phenotype in Sorsby's fundus dystrophy. *J Biol Chem.* 2000;35: 27027–27031.
40. Felbor U, Stohr H, Amann T, Schonherr U, Weber BH. A novel Ser156Cys mutation in the tissue inhibitor of metalloproteinases-3 (TIMP3) in Sorsby's fundus dystrophy with unusual clinical features. *Hum Mol Genet.* 1995;12:2415–2416.
41. Umeda S, Ayyagari R, Suzuki MT, et al. Molecular cloning of ELOVL4 gene from cynomolgus monkey (Macaca fascicularis). *Exp Anim.* 2003;2:129–135.
42. Edwards AO, Donoso LA, Ritter R III. A novel gene for autosomal dominant Stargardt-like macular dystrophy with homology to the SUR4 protein family. *Invest Ophthalmol Vis Sci.* 2001;11:2652–2663.
43. Wienberg J, Stanyon R. Comparative painting of mammalian chromosomes. *Curr Opin Genet Dev.* 1997;6:784–791.
44. O'Brien SJ, Menotti-Raymond M, Murphy WJ, et al. The promise of comparative genomics in mammals. *Science.* 1999;5439:458–462,479–481.
45. Crouau-Roy B, Service S, Slatkin M, Freimer N. A fine-scale comparison of the human and chimpanzee genomes: linkage, linkage disequilibrium and sequence analysis. *Hum Mol Genet.* 1996;8: 1131–1137.

Available online at www.sciencedirect.com
SCIENCE DIRECT®
Molecular Genetics and Metabolism 82 (2004) 173–179
Molecular Genetics and Metabolism
www.elsevier.com/locate/ymgme

Genitourinary phenotype in XX patients with distal 9p monosomy

Yoko Fujimoto,[a,b,c] Torayuki Okuyama,[d] Makoto Iijima,[e] Toshiaki Tanaka,[f] Reiko Horikawa,[c] Koichiro Yamada,[b] and Tsutomu Ogata[a,*]

[a] *Department of Endocrinology and Metabolism, National Research Institute for Child Health and Development, Tokyo, Japan*
[b] *Department of Pediatrics, Shouwa University School of Medicine Fujigaoka Hospital, Yokohama, Japan*
[c] *Division of Adolescent and Young Adult Medicine, National Center for Child Health and Development, Tokyo, Japan*
[d] *Division of Clinical Genetics and Molecular Medicine, National Center for Child Health and Development, Tokyo, Japan*
[e] *Division of Nephrology, National Center for Child Health and Development, Tokyo, Japan*
[f] *Division of Endocrinology and Metabolism, National Center for Child Health and Development, Tokyo, Japan*

Received 30 January 2004; received in revised form 5 April 2004; accepted 5 April 2004
Available online 8 May 2004

Abstract

Although testicular development has been shown to be variably impaired in XY patients with distal 9p monosomy, ovarian and other genitourinary phenotype has poorly been studied in XX patients monosomic for the distal 9p region. Thus, we studied a 13-month-old infant with 46,XX,der(9)t(9;10)(p23;p13) (case 1) and an 11-year-old girl with 46,XX,der(9)t(9;16)(p23;q22) (case 2). Case 1 had primary hypogonadism (basal serum follicle stimulating hormone [FSH], 40.0 mIU/mL; leteinizing hormone [LH], 1.2 mIU/mL; estradiol [E_2], <10 pg/mL), whereas case 2 had age-appropriate pubertal development (breast, Tanner stage 4; pubic hair, Tanner stage 3; menarche 11.7 years of age) and hormone values (FSH, 7.3 mIU/mL; LH, 6.7 mIU/mL; E_2, 47 pg/mL). In addition, case 1 had hypoplastic labia majora, short distance between the vaginal orifice and the anus, and five renal cysts, and case 2 had anal atresia, short distance between the vaginal orifice and the anus, bilateral hydronephrosis of grade 3 with probable ureteropelvic junction stenosis, and renal dysfunction (serum creatinine, 1.52 mg/dL; urea nitrogen, 34.5 mg/dL). Fluorescence in situ hybridization analysis for five regions and microsatellite analysis for 10 loci on 9p confirmed hemizygosity for the distal 9p region with the breakpoints between *IFNA* and *D9S285* in case 1 and between *D9S168* and *D9S286* in case 2. The results, in conjunction with the previous data in XX patients with molecularly defined distal 9p monosomy, are consistent with the presence of a gene(s) involved in the development of indifferent gonad or subsequent ovarian differentiation in a ~11 Mb region distal to *D9S168*. In addition, it is possible that a gene(s) for anoperineal and renal development also maps distal to *D9S168* and that for external genital development maps distal to *D9S285* at the position ~16 Mb from the 9p telomere.

Keywords: 9p monosomy; Sex determination; Ovarian development; Genitourinary development; Penetrance

Introduction

Testicular development has been shown to be variable from nearly normal testis formation to nearly complete gonadal dysgenesis or agenesis in XY patients with distal 9p monosomy [1–3]. Since the degree of impaired testis development is independent of the deletion size, it has been suggested that a gene(s) for testis development resides in the 9p monosomic region shared by the patients with defective testis development, and that haploinsufficiency of the gene(s) leads to various degrees of impaired testis formation [1–3]. Although the gene(s) for testis development has not been identified, it has has been localized to a terminal ~700 kb region distal to the exons of *DMRT1* (doublesex and mab-3 related transcription factor 1), on the basis of molecular studies in XY sex reversed patients with distal 9p monosomy [2]. The relevance of epigenetic imprinting is unlikely, because impaired male sex development can occur regardless of the parental origin of deleted 9p chromosomes [3].

* Corresponding author. Fax: +81-3-5431-6057.
E-mail address: tomogata@nch.go.jp (T. Ogata).

1096-7192/$ - see front matter © 2004 Elsevier Inc. All rights reserved.
doi:10.1016/j.ymgme.2004.04.003

However, ovarian phenotype has poorly been studied in XX patients hemizygous for the distal 9p region. In addition, other genitourinary findings have also poorly been examined in patients with distal 9p monosomy. Here, we report on two Japanese XX patients monosomic for the distal 9p region, and discuss on ovarian and other genitourinary development in distal 9p monosomy.

Case reports

Case 1

This female infant was the 2.92 kg (−0.5 SD) product of an uncomplicated term pregnancy. The parents were non-consanguineous and healthy. Shortly after birth, she was referred to our hospital because of multiple minor anomalies. Physical examination showed a feeble and hypopigmented infant with various dysmorphic features indicative of 9p monosomy syndrome, such as trigonocephaly, up-slanting palpebral fissures, flat nasal ridge, small and deformed ears, high arched palate, micrognathia, and bilateral short second and third fingers. External genitalia were feminized with hypoplastic labia majora. The distance between the vaginal orifice and the anus appeared to be diminished. There were no major anomalies. Thereafter, she had developmental retardation: she controlled her head at 6 months of age and sat without support at 12 months of age.

At 13 months of age, she was evaluated for genitourinary development. Biochemical studies indicated primary hypogonadism (Table 1) and normal renal function with serum creatinine of 0.29 mg/dL (age-matched normal range, 0.3–0.6 mg/dL) and urea nitrogen of 10.0 mg/dL (7.4–19.1 mg/dL) [6]. Abdominal ultrasound examinations showed rudimentary uterus and failed to detect gonadal structures. Renal size was normal (the maximum renal length, 7.3 cm for the right kidney and 7.2 cm for the left kidney) (height-matched reference data, 5.2–7.8 cm) [9] as was renal echogenicity, but five simple cysts of 3–6 mm in diameter were detected in the right renal cortex. At present, she is 17 months old, measures 79.1 cm (+0.2 SD), and weighs 9.35 kg (−0.5 SD).

Case 2

This girl was a cousin of the previously reported female infant with 46,XX,der(9)t(9;16)(p23;q22) (case 3 in Table 1) [3]; the father of case 2 was the younger brother of the father of case 3 who had 46,XY,t(9;16)(p23;q22). The parents of case 2 were non-consanguineous and healthy, as were the parents of case 3. Case 2 was also found to have chromosomal abnormality involving 9p at another hospital.

At $11\frac{2}{12}$ years of age, she came to our hospital with her mother, asking appropriate examination and management. Allegedly, she had anal atresia that was surgically treated at four months of age, cleft palate that was repaired at 6 months of age, and sensory deafness that was diagnosed by auditory brainstem response at 18 months of age. She was repeatedly affected with intractable otitis media that often required hospitalization, and routine laboratory tests at the time of admissions indicated gradual increase in serum creatinine level from ~6 years of age. She had severe developmental retardation and attended a special school for mentally delayed children.

Physical examination revealed various minor anomalies consistent with 9p monosomy syndrome, such as trigonocephaly, up-slanting palpebral fissures, large nose, flat nasal ridge, short anteverted nostrils, long philtrum, high arched palate, and distal symphalangism of the bilateral 2nd–5th fingers. External genitalia were those of normal girls, and the distance between the vaginal orifice and the anus appeared to be shortened. She exhibited breast development at Tanner stage 3 and pubic hair development at Tanner stage 2 (Japanese reference data: breast stage 3, 11.6 ± 1.5 years; pubic hair stage 2, 11.7 ± 1.6) [8]. Biochemical studies indicated normal pituitary-gonadal function (Table 1), and impaired renal function with increased serum creatinine of 1.52 mg/dL (0.4–0.8 mg/dL), urea nitrogen of 34.5 mg/dL (6.9–18.5 mg/dL), and uric acid of 8.0 mg/dL (2.5–6.0 mg/dL) [6]. Abdominal ultrasound examinations delineated moderately enlarged uterus and ovary-like structures. Renal size was normal (the maximum renal length, 7.5 cm for the right kidney, and 7.2 cm for the left kidney) (height-matched normal range, 7.0–9.6 cm) [9], but hydronephrosis of grade 3 with probable ureteropelvic junction stenosis was delineated bilaterally. Furthermore, the echogenicity was stronger in the renal cortex that in the liver, suggesting renal dysplasia. Thus, periodical examinations were recommended.

At 11.7 years of age, she experienced menarche, and exhibited breast development at Tanner stage 4 and pubic hair development at Tanner stage 3 (Japanese reference data: menarche, 12.25 ± 1.25 years; breast stage 4, 13.3 ± 1.5 years; pubic hair stage 3, no data) [8]. At present, she is $11\frac{9}{12}$ years old, measures 123.1 cm (−4.3 SD), and weighs 28.4 kg (−1.5 SD).

Methods

Conventional and molecular cytogenetic studies

After obtaining written informed consent, peripheral blood was obtained from case 1 and her parents and from case 2. Chromosome analysis was performed on 50 peripheral lymphocytes with G-banding. Fluorescence in situ hybridization (FISH) analysis was carried out for lymphocyte metaphase spreads, with a bacterial artificial chromosome (BAC) probe containing the marker *305J7-T7* (41-L13), a yeast artificial chromosome (YAC) probe

Table 1
Ovariand and other genitourinary findings in karyotypic female patients with molecularly defined distal 9p monosomy

Case	Age (y:m)	E_2[a] (pg/mL)	FSH[a] (mIU/mL)	LH[a] (mIU/mL)	Tanner stage	Menarche (years)	Fertility	Gonadal histology	Müllerian derivatives	External genitalia	Anoperineal region	Renal region
1	1:02	<10 (<10)	40.0 (1.6–5.7)	1.2 (<1.0)	B1, P1	—	—	N.E.	Uterus	Hypoplastic labia majora	Short A–V length	Cystic lesions ($n = 5$)
2	11:08	47 (<10–120)	7.3 (1.1–8.7)	6.7 (0.3–8.1)	B4, P3	11.7 (12.25 ± 1.25)	—	N.E.	Uterus	Normal	Anal atresia short A–V length	Hydronephrosis renal dysfunction
3[b]	1:05	12 (<20)	41.0 (1.6–5.7)	2.0 (<1.0)	B1, P1	—	—	N.E.	Uterus	Normal	Anal atresia	Normal
	5:09	<10 (<10)	17.1 (0.3–3.8)	0.7 (<1.0)	B1, P1							
4	2:04	<10 (<10)	7.6 (1.6–5.7) Peak, 38.2[e] (2.2–16.4)	0.6 (<1.0) Peak, 9.4[e] (2.6–4.7)	B1, P1	—	—	N.E.	Uterus	Normal	Normal	Normal
5[c]	11:08	43 (<10–130)	7.2 (1.5–6.0)	3.9 (0.1–2.5)	B4, P2	10.8 (12.25 ± 1.25)	—	N.E.	Uterus	Hypoplastic labia majora	Normal	Normal
6	Fetus (24 weeks)	—	—	—	—	—	—	Normal	Normal	Normal	Normal	Normal
7[d]	Adult	N.E.	N.E.	N.E.	N.E.	N.E.	Yes	N.E.	N.E.	N.E.	N.E.	N.E.

References: cases 1 and 2 (this report); case 3, Muroya et al. [3] (case 6 in [3]); cases 4 and 5, Ogata et al. [4] (cases 2 and 1 in [4], respectively); case 6, Vialard et al. [5]; and case 7, Calvari et al. [2].
E_2: estradiol, FSH: follicle stimulating hormone; LH: luteinizing hormone; B: breast; P: pubic hair; N.E.: not examined; and A–V: the anus to the vaginal orifice.
The values in parentheses for Japanese cases 1–5 represent age- and sex-matched Japanese reference data [6–8].
[a] Basal serum hormone values.
[b] The cousin of case 2; case 3 has been reported at $1\frac{5}{12}$ years of age, and endocrine data obtained at $5\frac{9}{12}$ years of age are also shown.
[c] Case 5 has been described at $8\frac{1}{12}$ years of age, and the latest unpublished data are shown in this Table.
[d] Case 7 has produced two 46,XY sex reversed patients with a submicroscopic distal 9p monosomy.
[e] Peak values in a gonadotropin releasing homone test (100 μg/m^2 bolus i.v.; blood sampling at 0, 30, 60, 90, and 120 min).

containing *D9S1779* (757A1), a YAC probe containing *D9S1858* (765H2), a BAC probe containing *DMRT1* (DMRT1/BAC), and a P1 phage artificial chromosome (PAC) probe containing *D9S1136* (34H2), together with a BAC probe for *APBA1* at 9q13–21 used as an internal signal control [3,10–12]. The probe for *APBA1* was labeled with biotin and detected by avidin conjugated to fluorescein isothiocyanate, and the remaining probes were labeled with digoxigenin and detected by rhodamine anti-digoxigenin.

Microsatellite analysis

Leukocyte genomic DNA of case 1 and her parents and of case 2 was amplified by polymerase chain reaction (PCR) with fluorescently labeled forward primers and unlabeled reverse primers defining 10 loci on 9p (Table 2). The primer sequences and the PCR conditions were as described in Genome Database (http://www.gdb.org). The PCR products were determined for the fragment size on an autosequencer (ABI PRISM 310), using GeneScan software 2.1. In addition, leukocyte genomic DNA of the cousin of case 2 (case 3 in Table 1) and the uncle of case 2 (the father of case 3), that had been collected previously [3], was similarly analyzed with permission.

Results

Conventional and molecular cytogenetic studies

The karyotype was 46,XX,der(9)t(9;10)(p23;p13) in case 1, 46,XX,t(9;10)(p23;p13) in her mother, and 46,XY in her father. Case 2 had a 46,XX,der(9)t(9;16)(p23;q22) karyotype, as did her cousin (case 3).

Representative FISH results are shown in Fig. 1A, and the data are summarized in Table 2. The 9p regions defined by the five probes were deleted from the abnormal chromosome 9 and preserved on the normal chromosome 9 in cases 1 and 2. In the mother of case 1, the corresponding regions were identified on the der(10) chromosome as well as on the normal chromosome 9, thereby confirming the translocation. The data of the cousin and the uncle of case 2 were based on the previous studies [3].

Microsatellite analysis

Representative results are shown in Fig. 1B, and the data are summarized in Table 2. In case 1, maternal alleles for *D9S1779*, *D9S288*, and *D9S285* were not inherited by the patient, while paternal alleles for the three loci were transmitted to the patient. For *IFNA*, *D9S169*, and *D9S165*, both maternal and paternal alleles were transmitted to the patient. Thus, it was shown that the abnormal chromosome 9 of cases 1 was of maternal origin and missing a distal 9p region with the breakpoint between *IFNA* and *D9S285*.

In case 2, two alleles were detected for *D9S168*, *D9S169*, and *D9S165*, and single alleles only were identified for the remaining seven loci. No allele common to the patient and her cousin was identified for *D9S1779* and *D9S288*. The cousin of case 2 did not inherit paternal alleles for *D9S288* and *D9S286*. Collectively, since the 9p breakpoint should be identical between case 2 and her cousin, it was determined to

Table 2
The results of FISH and microsatellite analysis

Locus/region	Chromosoma location	Methods	Case 1			Case 2		
			Father	Patient	Mother	Patient	Cousin[a]	Uncle[a,b]
41-L13/BAC	9p24.3	FISH	Two copies	Single copy	Two copies[c]	Single copy	Single copy	Two copies[c]
D9S1779	9p24.3	MS	121, 123	123	143, 145	135[c]	141	137, 141
757A1/YAC	9p24.3	FISH	Two copies	Single copy	Two copies[c]	Single copy	Single copy	Two copies[c]
765H2/YAC	9p24.3	FISH	Two copies	Single copy	Two copies[c]	Single copy	Single copy	Two copies[c]
DMRT1/BAC	9p24.3	FISH	Two copies	Single copy	Two copies[c]	Single copy	Single copy	Two copies[c]
D9S129	9p24.3	MS	128	128	128, 130	130	130	128, 130
34H2/PAC	9p24.3–p24.1	FISH	Two copies	Single copy	Two copies[c]	Single copy	Single copy	Two copies[c]
D9S1871	9p24.3–p24.1	MS	140, 142	142	140, 142	142	142	142, 148
D9S288	9p24.3–p24.1	MS	120, 134	134	120, 124	140[d]	124	128, 130
D9S286	9p23	MS	153, 155	153	153	157[d]	157	153, 155
D9S168	9p23	MS	232	232	226, 232	226, 236	226	226, 232
D9S285	9p22	MS	120	120	104, 118	120	120	112, 120
IFNA	9p22	MS	141, 147	143, 147	143, 149	147	141, 147	141, 147
D9S169	9p21.1	MS	267	257, 267	257, 261	261, 267	261, 263	257, 261
D9S165	9p21.1	MS	212	212, 218	208, 218	211, 215	207, 211	211, 213

BAC: bacterial artificial chromosome; YAC: yeast artificial chromosome; PAC: P1 phage artificial chromosome; FISH: fluorescence in situ hybridization analysis; and MS: microsatellite analysis. The locus/region order and the chromosomal location are based on the previous reports [2,13,14]. The Arabic numbers for microsatellite analysis indicate the sizes of fragments produced by polymerase chain reaction (bp).

[a] The microsatellite results are obtained in this study, and the FISH data are based on the previous report [3].

[b] The father of the cousin.

[c] One signal on the normal chromosome 9, and the other signal on the translocated chromosome involving the distal 9p.

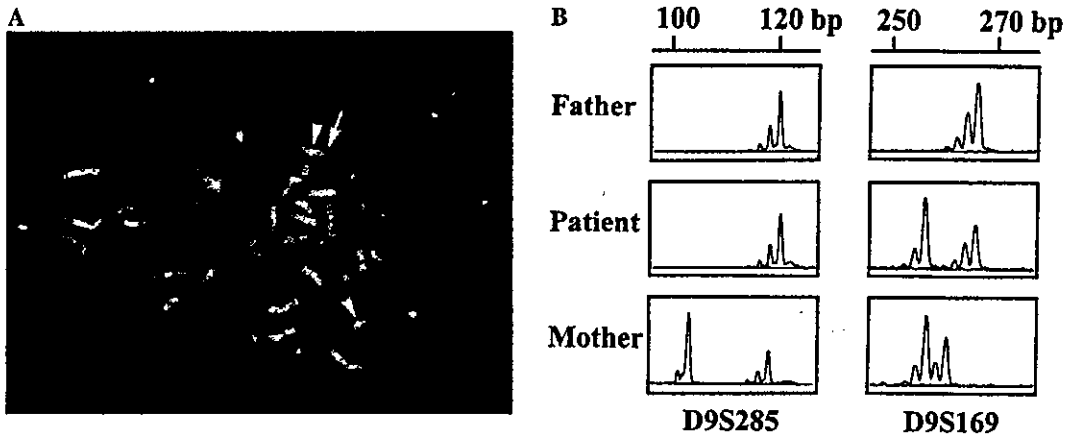

Fig. 1. (A) Representative FISH analysis in case 1. Only a single signal is detected for *DMRT1* (arrows), whereas two signals are found for *APBA1* used as an internal signal control (arrowheads). (B) Representative microsatellite results in case 1. For *D9S285*, the paternal allele only is transmitted to the patient and the maternal alleles are not inherited by the patient, demonstrating hemizygosity of this locus in the patient. For *D9S169*, the patient is heterozygous with the paternally and maternally derived alleles.

reside between *D9S168* and *D9S286* in case 2 and her cousin.

Discussion

Ovarian and other genitourinary development was different between cases 1 and 2 with molecularly confirmed distal 9p monosomy. Case 1 had hypergonadotropic hypogonadism consistent with ovarian dysfunction, together with external genital, anoperineal, and renal lesions. Case 2 had menarche and age-appropriate pubertal development indicative of normal ovarian function, and manifested anoperineal and renal lesions. The FSH dominant hypergonadotropinism in case 1 would primarily be due to her young age, because primary ovarian dysfunction is usually manifested by FSH dominant hypergonadotropinism in prepubertal girls and by elevation of both FSH and LH in pubertal to adult females [15,16]. Thus, although the effects of extra chromosomal materials translocated onto distal 9p can not be excluded, the results suggest that ovarian and other genitourinary development is variably impaired in XX patients with distal 9p monosomy.

Ovarian and other genitourinary phenotype has been reported in a total of seven karyotypic female patients with molecularly defined distal 9p monosomy (Table 1) (this report and [2–5]). Ovarian function is highly variable, including overt primary hypogonadism in cases 1 and 3, borderline hypergonadotropinism in case 4, normal histological findings in case 6, positive menses in cases 2 and 5, and proven fertility in case 7. Such diverse ovarian development in XX patients is consistent with the presence of a gene(s) involved in the development of indifferent gonad common to both sexes or subsequent ovarian differentiation specific to females. Furthermore, external genital, anoperineal, and renal abnormalities are exhibited by some of the seven cases. This would suggest the presence of a gene(s) for genitourinary development on distal 9p. In support of this, external genital and anoperineal lesions have often been described in XX patients with distal 9p deletions, and renal lesions have occasionally been reported in XX and XY patients with distal 9p deletions, although molecular studies have not been performed in such patients [17–20].

The deletion maps of the seven cases are shown in Fig. 2, together with the karyotypes. Several points should be made with respect to genoype-phenotype correlations. First, haploinsufficiency of genes involved in human development is usually associated with a wide range of penetrance and expressivity, probably depending on other genetic and environmental factors [21]. Indeed, male sex development is highly variable in XY patients with distal 9p monosomy [3,17]. Second, as indicated by the development of renal dysfunction from ~6 years of age in case 2, several features could be age-dependent, so that they may be unrecognized if not assessed at an appropriate age. Third, some features such as renal lesion would be overlooked without appropriate examinations. These points imply that the absence of a specific feature does not warrant the preservation of a relevant gene, while the presence of a specific feature indicates loss of a relevant gene.

Thus, deletion mapping should primarily be based on the results in patients with clinically discernible phenotype. In this context, the gene(s) for ovarian development as well as that for anoperineal and renal development would be located to a roughly 11 Mb region distal to *D9S168*, and that for external genitalia development to an approximately 16 Mb distal to *D9S285*, on the basis of ovarian dysfunction in cases 1 and 3, external genital abnormality in cases 1 and 5, anoperineal lesion in cases 1–3, and renal lesion in cases 1 and 2 (Table 1). Lack of abnormal phenotype in cases

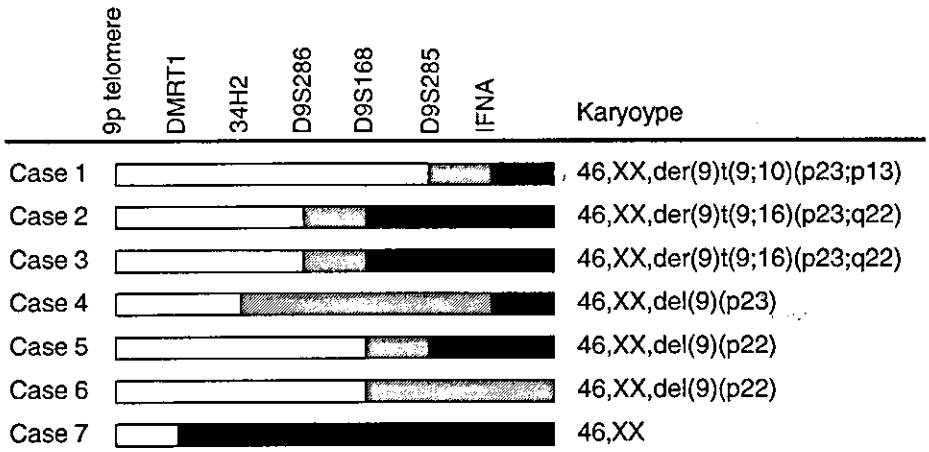

Fig. 2. Deletion maps and karyotypes of the seven patients with molecularly defined distal 9p monosomy. The case numbers correspond to those in Table 1. Of multiple loci examined in each case, the loci defining the breakpoint only are shown. The white and the black areas denote the monosomic and the disomic regions, respectively, and the striped areas depict the dosage unknown regions where the breakpoints should exist. According to the Ensembl Genome Browser at the Sanger Institute (http://www.ensembl.org/), the physical distance from the 9p telomere is roughly ~0.75 Mb for *DMRT1*, ~2.8 Mb for *34H2* (*D9S1136*), ~8.0 Mb for *D9S286*, ~10.6 Mb for *D9S168*, ~16.0 Mb for *D9S285*, and ~21 Mb for *IFNA*.

missing the critical regions would be explained by assuming incomplete penetrance. In particular, since the extent of ovarian and other genitourinary development is obviously different in related cases 2 and 3 who should have the identical size of 9p deletion, this argues for a wide range of penetrance. It may be possible, however, that another gene(s) for ovarian development or fertility and that for other genitourinary development reside in the more proximal region. Furthermore, it remains to be determined whether the gene(s) for ovarian development and that for other genitourinary development is identical or different, as is the gene(s) for ovarian development and that for testicular development.

Of multiple genes mapped on the critical regions defined in this study, *KANK* (kidney ankyrin repeat-containing protein) and *DMRT2* (doublesex and mab-3 related transcription factor 2) may be noteworthy. *KANK* is present at the position ~500 kb from the 9p telomere (distal to *DMRT1*) and is strongly expressed in the ovary [22], and *DMRT2* is present at the position ~1000 kb from the 9p telomere (proximal to *DMRT1*) and is strongly expressed in the kidney [23,24]. Thus, while detailed studies have not been performed, *KANK* and *DMRT2* could be regarded as candidate genes for ovarian and renal development, respectively. Although *Dmrt1*, a murine homolog for *DMRT1*, is expressed in the developing indifferent gonad [25], *DMRT1* is unlikely to be relevant to ovarian development: *Dmrt1* is most strongly expressed in the male-specific developing testis [25], and *Dmrt1* knockout XX mice have normal ovary, though *Dmrt1* knockout XY mice have defective testis development [26]. In addition, although the distal 9p region harbors *OVC* (ovarian adenocarcinoma oncogene), *OVC* is assigned between *IFNA* and *D9S169* and, therefore, maps outside the critical region defined in this study [27].

Cases 1–6 had a constellation of minor anomalies consistent with 9p monosomy syndrome [17]. In this regard, the critical region for 9p monosomy syndrome has been postulated between *D9S168* and *D9S144* by Veitia et al. [28] and between *D9S285* and *D9S286* by Christ et al. [29] (the locus order: 9p telomere–*D9S286*–*D9S144*–*D9S168*–*D9S285*–9p centromere), while the precise interval of the critical region and the number of relevant genes remain to be clarified. The 9p monosomy syndrome phenotype in cases 1–6 would primarily be compatible with the previously suggested location of the critical region for 9p monosomy syndrome.

In summary, the present study suggests that distal 9p monosomy results in not only variable degrees of impaired testicular development, but also diverse extent of defective ovarian and other genitourinary development. However, this notion remains speculative at present especially with regard to ovarian development, because the assessment of ovarian dysfunction in cases 1 and 3 is based on endocrine data only. Further studies will serve to define ovarian and other genitourinary phenotype in distal 9p monosomy, and to isolate the relevant gene(s).

Acknowledgments

This work was supported by a grant for Child Health and Development from the Ministry of Health, Labor, and Welfare (14C-1), and by a Grant-in-Aid from the Ministry of Education, Science, Sports, and Culture (15591150).

References

[1] C. Ottolenghi, K. McElreavey, Deletion of 9p and the quest for a conserved mechanism of sex determination, Mol. Genet. Metab. 71 (2000) 397–404.

[2] V. Calvari, V. Bertini, A. De Grandi, G. Peverali, O. Zuffardi, M. Ferguson-Smith, J. Knudtzon, G. Camerino, G. Borsani, S. Guioli, A new submicroscopic deletion that refines the 9p region for sex reversal, Genomics 65 (2000) 203–212.

[3] K. Muroya, T. Okuyama, K. Goishi, Y. Ogiso, S. Fukuda, J Kameyama, H. Sato, Y. Suzuki, H. Terasaki, H. Gomyo, K. Wakui, Y. Fukushima, T. Ogata, Sex determining gene(s) on distal 9p: clinical and molecular studies in six cases, J. Clin. Endocrinol. Metab. 85 (2000) 3094–3100.

[4] T. Ogata, K. Muroya, H. Ohashi, H. Mochizuki, T. Hasegawa, M. Kaji, Female gonadal development in XX patients with distal 9p monosomy, Eur. J. Endocrinol. 145 (2001) 613–617.

[5] E. Vialard, C. Ottolenghi, M. Gonzales, A. Choiset, S. Girard, J.P. Siffroi, K. McElreavey, C. Vibert-Guigue, M. Sebaoun, N. Joye, M.F. Portnoi, F. Jaubert, M. Fellous, Deletion of 9p associated with gonadal dysfunction in 46, XY but not in 46, XX human fetuses, J. Med. Genet. 39 (2002) 514–518.

[6] Japan Public Health Association, Normal biochemical values in Japanese children, Sanko Press, Tokyo, 1996 (in Japanese).

[7] J. Ito, T. Tanaka, R. Horikawa, Y. Okada, S. Morita, M. Koitaji, A. Tanae, I. Hibi, Serum LH and FSH levels during GnRH tests and sleep in children, J. Jpn. Pediatr. Soc. 97 (1993) 1789–1796, in Japanese.

[8] N. Matsuo, Skeletal and sexual maturation in Japanese children, Clin. Pediatr. Endocrinol. 2 (Suppl.) (1993) 1–4.

[9] B.K. Han, D.S. Babcock, Sonographic measurements and appearance of normal kidneys in children, AJR 145 (1985) 611–616.

[10] W.L. Flejter, J. Fergestad, J. Gorski, T. Varvilli, S. Chandrasekharappa, A gene involved in XY sex reversal is located on chromosome 9, distal to marker D9S1779, Am. J. Hum. Genet. 63 (1998) 794–802.

[11] Y. Ning, A. Roschke, A.C.M. Smith, M. Macha, K. Precht, H. Riethman, D.H. Ledbetter, J. Flint, S. Horsley, R. Regan, L. Kearney, S. Knight, K. Kvaloy, W.R.A. Brown, A complete set of human telomeric probes and their clinical application, Nat. Genet. 14 (1996) 86–89.

[12] S.J.L. Knight, C.M. Lese, K.S. Precht, J. Kuc, Y. Ning, S. Lucas, R. Regan, M. Brenan, A. Nicod, N.M. Lawrie, D.L. Cardy, H.T.J. Nguyen, H.C. Riethman, D.H. Ledbetter, J. Flint, An optimized set of human telomere clones for studying telomere integrity and architecture, Am. J. Hum. Genet. 67 (2000) 320–332.

[13] M. Bouzyk, S.P. Bryant, C. Evans, S. Guioli, S. Ford, K. Schmidt, P.N. Goodfellow, S. Povey, M. Rebello, S. Rousseaux, N.K. Spurr, Integrated radiation hybrid and yeast artificial chromosome map of chromosome 9p, Eur. J. Hum. Genet. 5 (1997) 299–307.

[14] S. Povey, J. Attwood, B. Chadwick, J. Frezal, J.L. Hains, M. Knowles, D.J. Kwiatkowski, O.I. Olopade, S. Slaugenhaupt, N.K. Spurr, M. Smith, K. Steel, J.A. White, M.A. Pericak-Vance, Report of the fifth international workshop on chromosome 9, Ann. Hum. Genet. 61 (1997) 183–206.

[15] R. Illig, M. Tolksdorf, G. Mürset, A. Prader, LH and FSH response to synthetic LH-RH in children and adolescents with Turner's and Klinefelter's syndrome, Helv. Paediatr. Acta 30 (1975) 221–231.

[16] J.L. Ross, D.L. Loriaux, G.B. Cutter Jr., Developmental changes in neuroendocrine regulation of gonadotropin secretion in gonadal dysgenesis, J. Clin. Endocrinol. Metab. 57 (1983) 288–293.

[17] J.L. Huret, C. Leonard, B. Forestier, M.O. Rethoré, J. Lejeune, Eleven new cases of del (9p) and features from 80 cases, J. Med. Genet. 25 (1988) 741–749.

[18] V. Shashi, W.L. Golden, J.S. Fryburg, Choanal atresia in a patient with the deletion (9p) syndrome, Am. J. Med. Genet. 49 (1994) 88–90.

[19] R. Ion, L. Telvi, J.L. Chaussain, J.P. Barbet, M. Nunes, A. Safar, M.O. Rethore, M. Fellous, K. McElreavey, Failure of testicular development associated with a rearrangement of 9p24.1 proximal to the SNF2 gene, Hum. Genet. 102 (1998) 151–156.

[20] R.A. Pfeiffer, A. Rauch, U. Trautmann, H.G. Dorr, O. Hiort, G. Scherer, G. Rosch, T. Papadopoulos, K. Hardt, E. Lachmann, Defective sexual development in an infant with 46,XY,der (9)t (8;9) (q23.1;p23)mat, Eur. J. Pediatr. 158 (1999) 213–216.

[21] E. Fisher, P. Scambler, Human haploinsufficiency: one for sorrow, two for joy, Nat. Genet. 7 (1994) 5–7.

[22] T. Nagase, N. Seki, K. Ishikawa, A. Tanaka, N. Nomura, Prediction of the coding sequences of unidentified human genes. V. The coding sequences of 40 new genes (KIAA0161-KIAA0200) deduced by analysis of cDNA clones from human cell line KG-1, DNA Res. 29 (1996) 17–24.

[23] C. Ottolenghi, R. Veitia, L. Quintana-MurcL, D. Torchard, L. Scapoli, N. Souleyreau-Therville, J. Beckmann, M. Fellous, K. McElreavey, The region on 9p associated with 46, XY sex reversal contains several transcripts expressed in the urogenital system and a novel doublesex-related domain, Genomics 64 (2000) 170–178.

[24] C. Ottolenghi, R. Veitia, M. Barbieri, M. Fellous, K. McElreavey, The human doublesex-related gene, DMRT2, is homologous to a gene involved in somitogenesis and encodes a potential bicistronic transcript, Genomics 64 (2000) 179–186.

[25] C.S. Raymond, J.R. Kettlewell, B. Hirsch, V.J. Bardwell, D. Zarkower, Expression of Dmrt1 in the genital ridge of mouse and chicken embryos suggests a role in vertebrate sexual development, Dev. Biol. 215 (1999) 208–220.

[26] C.S. Raymond, M.W. Murphy, M.G. O'Sullivan, V.J. Bardwell, D. Zarkower, Dmrt1, a gene related to worm and fly sexual regulators, is required for mammalian testis differentiation, Genes Dev. 14 (2000) 2587–2595.

[27] G. Chenevix-Trench, J. Kerr, M. Friedlander, T. Hurst, B. Sanderson, M. Coglan, B. Ward, J. Leary, S.K. Khoo, Homozygous deletions on the short arm of chromosome 9 in ovarian adenocarcinoma cell lines and loss of heterozygosity in sporadic tumors, Am. J. Hum. Genet. 55 (1994) 143–149.

[28] R.A. Veitia, M. Nunes, L. Quintana-Murci, R. Rappaport, E. Thibaud, F. Jaubert, M. Fellous, K. McElreavey, J. Goncalves, M. Silva, J.C. Rodrigues, M. Caspurro, F. Boieiro, R. Marques, J. Lavinha, Swyer syndrome and 46, XY partial gonadal dysgenesis associated with 9p deletions in the absence of monosomy-9p syndrome, Am. J. Hum. Genet. 63 (1998) 901–905.

[29] L.A. Christ, C.A. Crowe, M.A. Micale, J.M. Conroy, S. Schwartz, Chromosome breakage hotspots and delineation of the critical region for the 9p-deletion syndrome, Am. J. Hum. Genet. 65 (1999) 1387–1395.

小児科診療〔第67巻・第8号〕別刷

2004年8月1日発行

発行所 株式会社 診断と治療社

特集　小児科医が知っておきたい眼科疾患

遺　伝

小須賀基通　奥山虎之　国立成育医療センター遺伝診療科

要旨

近年の分子生物学の進歩により，遺伝性眼疾患の責任遺伝子が同定され，その発症のメカニズムが解明されつつある．それに伴い遺伝性眼疾患に携わる医療従事者に対して，疾患の遺伝形式，再発危険率，遺伝子診断などの遺伝に関するさまざまな情報の提供が求められてきている．さらに，これらの遺伝情報をめぐるさまざまな倫理的問題の対応や心理的・社会的支援も含んだ遺伝カウンセリングの重要性が，今後ますます増していくものと思われる．

Key Words
遺伝カウンセリング
遺伝形式
遺伝性眼疾患
症候群性眼疾患
非症候群性眼疾患

0386-9806/04/¥100/頁/JCLS

はじめに

近年の分子生物学の進歩により，多くの疾患の責任遺伝子が同定されつつある．すでに一部の疾患では，その発症のメカニズムが解明され遺伝子検査による確実な診断が可能になった．それに伴い遺伝性疾患に携わる医療従事者にも，疾患の遺伝形式，再発危険率だけでなく遺伝子診断など遺伝に関するさまざまな情報の提供が求められるようになってきた．またこれらの遺伝情報をめぐるさまざまな倫理的問題も生じてきており，心理的・社会的支援をも含んだ遺伝カウンセリングの必要性が認識されつつある．

眼科疾患についても多くの責任遺伝子が同定され，従来の，視覚電気生理やその他の機能的検査では診断がつかなかった非典型的な眼科疾患も，遺伝子検査による確定診断が可能となった．ヒト遺伝子や遺伝性疾患のカタログであるOMIN（Online Mendelian Inheritance in Man）[1]によると，2004年2月現在，約15,000項目の遺伝子座や疾患が登録されており，そのうち約11,000が遺伝性疾患として分類されている．これらの遺伝性疾患のうち，眼病変を伴うものは約1,400と報告されている．

眼疾患の遺伝について説明する際，眼疾患の存在が単独で存在する非症候群性眼疾患か，あるいは合併症として存在する症候群性眼疾患で

あるか否かで，診断・予後・遺伝形式や再発危険率などがまったく違ったものになってしまう．したがって眼疾患を見た場合には，それ以外の全身性の合併症の存在を必ず念頭におくこと，あるいは疾患のひとつの合併症としての眼疾患の有無を見落とさないことがきわめて重要である．

本稿では，小児科医が日常の臨床の現場で遭遇する可能性が比較的高い，先天的あるいは小児期発症の眼科疾患の遺伝カウンセリングをする際に，留意すべき内容などについて説明する．

遺伝性疾患の分類と再発危険率

遺伝性疾患とは，遺伝子の変異が病因としてかかわる疾患である．それらは大別すると単一の遺伝子の変異が原因でおこる疾患（単一遺伝子病），ミトコンドリアDNAの異常によるミトコンドリア遺伝病，多因子遺伝病，染色体異常からなる．再発危険率とは，ある家系内に一人の患者がいた場合，同じ両親からその次の子が同じ疾患に罹患する確率であり，疾患の遺伝形式や疾患の浸透率によって決まる．遺伝子型の変異により表現型の異常が出現する確率を浸透率という．

1．常染色体優性遺伝

ヒトの常染色体は，父由来のものと母由来のものがそれぞれ1本ずつ伝わり計2本が存在する．したがって父由来と母由来の同じ遺伝子をそれぞれ一つ，計二つ保有している．その遺伝子のどちらか一方に変異がある場合に発症する遺伝形式を常染色体優性遺伝という．

両親のどちらかが罹患者で遺伝子変異を保有している場合，遺伝子変異が子に伝わり，同じ疾患に罹患する確率は男女を問わず50％となる．浸透率が低い疾患の場合は，両親のどちらかが遺伝子変異を保有していても発症していないこともある．また発症していても症状が軽く，本人に自覚症状がないこともある．その場合は児に遺伝子変異が伝わり，児が明らかな罹患者となってから，親の罹患が判明することもある．

また遺伝子変異を保有していない親から，配偶子の形成期に突然変異により遺伝子変異が生じて，児が罹患者になる突然変異例も認められる．この場合の次子再発危険率はきわめて低い．

2．常染色体劣性遺伝

常染色体劣性遺伝は，常染色体上に存在する一対二つの遺伝子の両方に変異を有する場合（ホモ接合体）に罹患者となり，一つに遺伝子変異があっても発症せずに保因者となる（ヘテロ接合体）．一般に両親が保因者の場合，子が罹患する確率は25％，子が親と同じ保因者になる確率が50％，まったく遺伝子変異が伝わらない確率が25％という計算になる．

3．X連鎖性劣性遺伝

女性はX染色体が2本存在し，X染色体上の遺伝子を対で保有している．したがって女性の場合，X染色体上の遺伝子の一方に変異があっても，対となっている一方の遺伝子が正常の場合，一般には発症せずに保因者となる．男性はX染色体が1本しか存在しないので，X染色体上の遺伝子に変異があれば罹患者となる．X連鎖性劣性遺伝の場合，保因者の女性と健康な男性との間では，子が遺伝子変異を受け継ぐ確率は男児，女児とも50％である．したがって女児は50％が保因者，50％が正常．男性は50％が罹患者，50％が正常である．

4．ミトコンドリア遺伝

エネルギー産生に関与する細胞質内小器官のミトコンドリアは，核内の遺伝子とは別に独自の遺伝子をもつ．このミトコンドリア遺伝子は，すべて卵子から由来し，母からのみ遺伝する（母系遺伝）．伝えられる変異ミトコンドリアDNAの細胞内，組織内における割合（ヘテロプラスミー）はさまざまであり，そのため遺伝したとしても，発症の程度もさまざまであるため，

再発危険率を正確に評価するのは困難である．

5．多因子遺伝

複数の遺伝子（遺伝要因）と環境要因の相互作用により発症すると考えられる疾患を多因子遺伝病とよぶ．生活習慣病，非症候群性の先天性心疾患や口蓋裂などは多因子遺伝と考えられる．遺伝様式はメンデルの遺伝法則に従わないため，再発危険率は疾患ごとの経験的再発危険率により推定する．

6．染色体異常

染色体異常には数的異常と構造異常がある．一般に数的異常は，配偶子形成の際の不分離という現象によって生じる．この場合，親が同様の数的異常をもつことはほとんどなく，再発危険率はきわめて低い．構造異常の場合は，親が均衡型相互転座を有することがあり，この場合は再発危険率を考慮しなければならない．

眼科疾患の遺伝

1．屈折異常

合併症を伴わない単純屈折異常は，環境要因と遺伝要因が関与する多因子遺伝形式である．

屈折異常を弱度の屈折異常（弱度近視）と，強度の屈折異常（強度近視）に分けると，弱度近視は環境要因の影響が大きく，強度近視は遺伝的要因の影響が大きい．合併症を伴わない強度近視は常染色体優性遺伝形式と考えられ，いくつかの原因遺伝子がすでに報告されている[2)3)]．とくに家系内に屈拙異常の罹患者が多い場合，浸透率が高いと考えられている．実際には他因子の影響も関係しているので屈折異常の再発危険率は4～5%程度と考えられている．

後述するStickler症候群やMarfan症候群などに合併する強度屈折異常は，浸透率がより高い常染色体優性遺伝形式をとる．

2．色覚異常

色覚異常のなかで，多いのは赤や緑の色合いが見分けにくくなる赤緑色覚異常（第一色覚異常と第二色覚異常）であり，これらはX連鎖性劣性遺伝形式をとる．一般の男性の約5%が罹患者で，女性の約10%が保因者である．

平成14年度までは学校健診の一部として色覚検査が行われていたが，平成15年度からは学校保健法の改定により，学校での色覚検査は必ずしも行わなくてもよい項目になった．本人が色覚異常を自覚していなくても日常生活に不便がなければ，色覚異常は，眼疾患というよりは色の見えかたの個性や体質であるともいえることから，家族や本人からの希望がなければ積極的な診断は不要とする考えもある．

一方，色の誤認を自覚できれば日常生活におこる不利益や混乱に対応できること，将来の進路を決める際には，色覚異常には一部の例外的な職業の就業の制限があること，家系内にほかに罹患者がいる場合は，家系内保因者の可能性があることから，自己決定が可能な年齢になった際や，挙児希望の場合には，積極的な診断や詳細な遺伝情報の提供は必要であるとする意見もある．

3．斜　視

ある家系内において斜視の発症が多く認められる事実が報告されており，遺伝性の斜視の存在は古くから指摘されている．

遺伝形式は常染色体優性遺伝，常染色体劣性遺伝，多因子遺伝のいずれも存在すると考えられる[4)]．とくにCongenital general fibrosis syndromeは，浸透率が比較的高い常染色体優性遺伝と考えられている．一般的には多因子遺伝が多いが，両親正常で斜視罹患の児が1人いる場合の再発危険率は約15%程度，両親のいずれかが罹患者の場合は約40%であると見積られている．

4．網膜芽細胞腫

網膜芽細胞種は，以前から小児期発症の遺伝性のがんとして知られており，全体の30%を占

める両眼性網膜芽細胞種はすべて遺伝性である．残りの70％の片眼性網膜芽細胞種のうち10～15％が遺伝性で，全体の55～60％は片眼性で非遺伝性であると考えられる．

常染色体優性遺伝の形式をとるが，浸透率は約90％であり遺伝子変異を受け継いでいても発症しない場合がある．13番染色体長腕14上に位置する癌抑制遺伝子のひとつである*RB*遺伝子が責任遺伝子である[5]．罹患者は二つの*RB*遺伝子に変異を生じている．遺伝性の場合は，配偶子の段階ですでに一つの*RB*遺伝子に変異が存在し，受精後の網膜形成期に，さらに一方の*RB*遺伝子に変異がおこり腫瘍化する．

非遺伝性の場合は，網膜細胞の分化，発達過程で二つの*RB*遺伝子に変異が生じて腫瘍化する（two hit theory）[6]．本症の5～6％の患者に13番染色体長腕14部分の欠失が認められる．この場合は，精神運動発達遅滞や外表奇形を伴う．

5．先天性緑内障

先天性緑内障は，約半数が出生時に約80％が1歳までに発症する．発生頻度は約1/10,000程度で，80％は特発性で20％が遺伝性と考えられる．原発性先天性緑内障は胎生期における前房隅角の形成異常が原因であり，ほかの眼疾患や全身性の合併症は有しないことが多い．常染色体劣性遺伝であるが，再発危険率は10％程度と考えられている．小児期発症の原発開放隅角緑内障の一部は原因遺伝子が同定されており，その場合は，常染色体優性遺伝形式をとる．実際はすべての原因が遺伝によるものではなく，他因子の影響もあるため，再発危険率は5～15％と考えられる．

いずれにしろ家族歴がある場合は，ない場合に比べて明らかに発生頻度が高くなるので，早期からの検査がすすめられる．Stickler症候群，Marfan症候群や無虹彩症などの，ほかの先天異常に合併しておこる続発性先天性緑内障は，これらの疾患の遺伝形式に従う．

6．先天性白内障

先天性白内障の20～30％は遺伝性で，30～50％は特発性である．母体内感染，奇形症候群，代謝異常症，染色体異常なども原因となる．

さまざまな原因遺伝子が報告されており，遺伝形式も常染色体優性遺伝，劣性遺伝形式が報告されている．先天性白内障の多くは常染色体優性遺伝である．とくに両眼性の場合は遺伝性の可能性があるため，児が両眼性の罹患者と診断された場合，家系内に明らかな罹患者がほかにいなくても両親や同胞の検査がすすめられる．

7．無虹彩症

発生頻度は約10万人に1人で，2/3が家族例で1/3は特発例と考えられる．11番染色体短腕13に位置する*PAX6*遺伝子の変異が原因であり[7]，常染色体優性遺伝形式をとる．家系内における無虹彩の表現型はさまざまであり，両側虹彩の完全欠損から虹彩の菲薄化を認めるだけの場合もある．したがって，自覚症状がなくても両親や同胞の眼疾患の有無についての精査が必要である．

無虹彩症の1/3にWilms腫瘍が合併するといわれており，同時に精神発達遅滞や尿道下裂，鼠径ヘルニアなどを合併している場合は，WAGR（Wilms tumor, aniridia, genitourinary abnormalies, mental retardation）症候群とよばれる[8]．この場合，多くの症例で11番染色体短腕13の欠失が認められ，*PAX6*遺伝子と近傍に位置する*WT1*遺伝子の欠失が原因である．したがって無虹彩症が認められた場合には，染色体検査（FISH法）を行い，11番染色体短腕13部分の欠失や，この部分を切断点とする染色体構造異常の有無を確認することが重要である．

8．レーベル視神経萎縮症

10歳代から20歳代にかけて，急性または亜急性の両眼性視力低下で発症する．患者の80％は男性患者である．ミトコンドリアDNAに点

突然変異がみられ，日本人の罹患者の約90％に共通の変異が認められる．しかし，遺伝子変異をもっていても男性では約40％，女性では約20％しか発症せず，また女性を介して遺伝するため，父親が罹患者の場合は遺伝しない．

再発危険率は，経験的再発危険率により母親が罹患者あるいは母親に症状はないが，前児が罹患者の場合，次子が男児の場合は約50％，女児の場合は約20％が罹患者となる．女児の約80％は保因者となる．小児期早期に発症する視神経萎縮症でレーベル視神経萎縮症と鑑別を要する疾患に，常染色体優性視神経萎縮があるが，本症は常染色体優性遺伝形式をとる．

9．症候群性眼疾患

眼疾患に加えて広範な合併症を伴う場合は，眼疾患を伴う症候群として診断され，単独の眼疾患とは違った遺伝形式や病態をとることがある．小児科診療で比較的受診する機会が多いと思われる眼疾患を伴う症候群について，遺伝性疾患について説明する．

1）Stickler症候群

強度の近視と小下顎，口蓋裂が特徴である．その他には関節症状や眼球の軽度突出などの特異顔貌，僧房弁逸脱，聴力障害などを伴うこともある．12番染色体上にマップされる*COL2A1*遺伝子が責任遺伝子である[9]．常染色体優性遺伝であるが，表現型には差があり，必ずしも家系内の罹患者は同様の症状をとるわけではない．児に口蓋裂，小下顎症による呼吸困難などのPierre Robin Sequenceを認めた場合には，屈折異常，白内障や網膜剝離など眼病変の有無を検査することをすすめる．また親にいずれかの症状があった場合は，よりいっそうStickler症候群の可能性を考える．

2）Marfan症候群

高身長，側彎・後彎など骨格異常，僧房弁逸脱・大動脈基部の拡張などの循環器病変，眼症状を伴う．眼症状は多くに近視を認め，50～80％に片側あるいは両側の水晶体変位を認める．染色体優性遺伝で浸透率は高いが，表現型には差があるため家系内の病歴や体型にも注意をはらう．

3）Goldenhar症候群（鰓弓症候群，眼・耳介・椎骨症候群）

同側の眼球類皮腫（デルモイド），片側の耳介変形（無耳，外耳道閉鎖から副耳のみまでさまざま），顔面の非対称などを呈し，一部の罹患者は椎骨の変形を伴う．頻度は5,000～25,000人に1人である．軽症例から重症例までさまざまであり，診断基準によって診断が左右される．ほとんどが特発例で多因子遺伝が考えられるが，まれに常染色体優性遺伝，常染色体劣性遺伝やX連鎖劣性遺伝を示す家系が存在する．特発例の場合，経験的再発危険率は2～3％である．

4）Lowe症候群（Oculo-cerebrorenal syndrome of Lowe）

両側の先天性白内障がほぼ必発し，その他，緑内障・角膜変性などの眼症状，新生児期の筋緊張低下，精神発達遅滞および腎尿細管性アシドーシスを呈する．X連鎖性劣性遺伝形式をとるが，まれに女児であっても症状を呈することがあるので注意を要する[10]．保因者の95％に眼病変が存在するため，眼病変有無は保因者診断に有用である．母親の眼病変を認めた場合は，次子再発危険率の情報提供が可能である．

5）ガラストース血症

ガラストース分解酵素の欠損などによる代謝異常のため，ガラストースや中間代謝産物が蓄積することで，白内障に加えて，嘔吐・下痢などの消化器症状や肝機能障害を呈する．新生児マス・スクリーニングの対象となっており，早期に発見されれば予後はよい．欠損酵素によりⅠ～Ⅲ型に分類されているが，いずれも責任遺伝子は同定されており，常染色体劣性遺伝形式をとるため再発危険率は25％である．

おわりに

遺伝性疾患の児をもった親は，多かれ少なかれ自責の念をもっており，また次子への再発を憂慮している．患者や家族から遺伝相談を求められた場合，単に遺伝形式や再発危険率などの遺伝情報を告げるだけではなく，これらの情報をもとに，患者や家族が遺伝にかかわる問題について，正しい自己決定ができるように援助することが必要である．

また，遺伝性疾患の遺伝子検査においては，検査目的とその結果の及ぼす影響について，医療者側も患者側もよく理解したうえで行うべきである．患者の確定診断や予後を推測するために行うのか，遺伝子検査の結果を用いて家系内での保因者診断，および出生前診断の応用まで念頭において行うのか，など検査の目的を明確にしておくべきである．そして検査の実施が，技術的・倫理的に可能であるのかについても，あらかじめよく検討すべきである．また必要に応じて適切な遺伝カウンセリングが受けられるように，施設の情報を提供しておくことも重要である．

●文　献

1) http://www.ncbi.nlm.nih.gov/entrez/query.fcgi?db=OMIM&tool=toolbar
2) Young TL, Ronan SM, Alvear AB et al.: A second locus for familial high myopia maps to chromosome 12q. Am J Hum Genet 63: 1419-1424, 1998
3) Young TL, Ronan SM, Alvear AB et al.: A genome wide scan for familial high myopia suggests a novel locus on chromosome 7q36. J Med Genet 39: 118-124, 2002
4) O'hara MA, Nelson LB: Heredity of strabismus 59. Biochemical foundation of ophthalmology, volume 3. Harper and Row, Philadelphia, 1993
5) Friend SH, Bernards R, Rogelj S et al.: A human DNA segment with properties of the gene that predisposes to retinoblastoma and osteosarcoma. Nature 323: 643-646, 1986
6) Knudson AG Jr: Mutation and cancer: statistical study of retinoblastoma. Proc Natl Acad Sci USA 68: 820-823, 1971
7) Hanson IM, Seawright A, Hardman K et al.: PAX6 mutations in aniridia. Hum Mol Genet 2: 915-920, 1993
8) Riccardi VM, Sujansky E, Smith AC: Chromosomal imbalance in the Aniridia-Wilms'tumor association: 11p interstitial deletion. Pediatrics 61: 604-610, 1978
9) Ahmad NN, Ala-Kokko L, Knowlton RG et al.: Stop codon in the procollagen II gene (*COL2A1*) in a family with the Stickler syndrome (arthro-ophthalmopathy). Proc Natl Acad Sci USA 88: 6624-6627, 1991
10) Hodgson SV, Heckmatt JZ, Hughes E et al.: A balanced de novo X/autosome translocation in a girl with manifestations of Lowe syndrome. Am J Med Genet 23: 837-847, 1986

著者連絡先

〒157-8535　東京都世田谷区大蔵2-10-1
国立成育医療センター遺伝診療科
小須賀基通

ARTICLE

doi:10.1016/S1525-0016(03)00262-4

Improvement of Skeletal Lesions in Mice with Mucopolysaccharidosis Type VII by Neonatal Adenoviral Gene Transfer

Arihiko Kanaji,[1,2,3] Motomichi Kosuga,[1,3,4] Xiao-Kang Li,[1] Yasuyuki Fukuhara,[1,3,4] Akiko Tanabe,[1] Yuko Kamata,[1,3] Noriyuki Azuma,[1,3] Masao Yamada,[1] Toyonori Sakamaki,[2,3] Yoshiaki Toyama,[2] and Torayuki Okuyama[1,3,4,*]

[1]*National Research Institute of Child Health and Development, Tokyo 157-8535, Japan*
[2]*Department of Orthopedics and* [4]*Department of Pediatrics, Keio University School of Medicine, Tokyo 160-8582, Japan*
[3]*National Center for Child Health and Development, Tokyo 157-8535, Japan*

**To whom correspondence and reprint requests should be addressed at the Department of Clinical Genetics and Molecular Medicine, National Center for Child Health and Development, 2-10-1 Okura Setagaya-ku, Tokyo 157-8535, Japan. Fax: +81-3-3416-2222. E-mail: okuyama-t@ncchd.go.jp.*

Neonatal gene transfer using adenovirus vectors expressing human β-glucuronidase (AxCAhGUS) resulted in pathological improvement in multiple visceral organs of mice with mucopolysaccharidosis type VII (MPSVII). However, the therapeutic effect on skeletal deformities and growth retardation, the major clinical symptoms in MPSVII, was not fully investigated by biochemical and histopathological analyses. In this study, we injected AxCAhGUS into a murine model of MPSVII (B6/MPSVII) within 24 h of birth and evaluated the therapeutic effects on skeletal deformities and growth retardation. High levels of β-glucuronidase (GUSB) activity (approximately threefold higher than normal GUSB activity) were observed in the articular cartilage of the mice 30 days after the treatment. Histopathological study in the knee joints showed elimination of vacuole cells in the articular cartilage and growth plate. Subchondral bone near the articular surface was almost normal in the treated MPSVII mice. Long-term observation (for 140 days after treatment) indicated that characteristic phenotypes such as flattened face, hunched stature, and shortening of bone length in the treated mice were almost normal. These results demonstrate that a single injection of adenovirus vector into neonatal MPSVII mice is sufficient for long-term normalization of skeletal deformities and effective in pathological correction of the articular cartilage and growth plate.

Key Words: mucopolysaccharidosis, adenovirus, skeletal lesions, gene therapy

INTRODUCTION

Mucopolysaccharidosis type VII (MPSVII, Sly disease)is a lysosomal storage disease caused by a deficiency of β-glucuronidase (GUSB) activity, which results in a progressive accumulation of undegraded glycosaminoglycans in the lysosomes [1]. MPSVII is characterized pathologically by lysosomal distension in many tissues and clinically by hepatosplenomegaly, mental and growth retardation, hearing and vision defects, skeletal deformities, and short life span [2].

B6/MPSVII is a murine model of MPSVII, sharing characteristic phenotypes and pathological abnormalities with human MPSVII [3–5]. In this model, a single base pair deletion in exon 10 of the GUSB gene results in the formation of a premature stop codon, leading to the complete absence of GUSB activity [3].

B6/MPSVII is a useful model to develop novel therapeutic approaches, such as enzyme replacement therapy (ERT) and bone marrow transplantation (BMT) [6–12]. In adult MPSVII mice, ERT and BMT will reverse visceral lesions and prolong survival, but have little effect on growth retardation, bone dysplasia, or lysosomal storage in the central nervous system [6,7]. In contrast, neonatal MPSVII mice receiving ERT or BMT showed an improvement in skeletal deformities [7,11,12]. Sands *et al.* reported on the therapeutic effect of BMT on skeletal deformities during the neonatal period [11]. They showed pathological improvement of the articular surface, growth

1525-0016/03 $30.00